



# Synthesis and fluorescence of dicyanoisophorone derivatives



Xu Zhang, Yi Chen\*

Key Laboratory of Photochemical Conversion and Optoelectronic Materials, Technical Institute of Physics and Chemistry, The Chinese Academy of Sciences, Beijing 100190, China

## ARTICLE INFO

### Article history:

Received 19 February 2013

Received in revised form

27 May 2013

Accepted 29 May 2013

Available online 20 June 2013

### Keywords:

Dicyanoisophorone derivatives

Fluorescence

Solid state

Stoke's shift

Substituent

Synthesis

## ABSTRACT

A class of dicyanoisophorone derivatives **1–5** with electron-donating groups has been prepared by a two-step condensation reaction. Fluorescence both in solution and in pure solid state are measured. It is found that dicyanoisophorone derivatives **1–5** exhibit fluorescence in both solution and pure solid state. An enhancement of fluorescence in solid state probably results from the aggregation-induced emission. It is also found that dicyanoisophorone derivatives **1–5** show large Stoke's shifts in solution as well as in pure solid state. The origin of fluorescence of dicyanoisophorone derivatives depends on the nature of substituents, with a strong push–pull chromophores dicyanoisophorone system, red or orange solid-state fluorescence is obtained.

© 2013 Elsevier Ltd. All rights reserved.

## 1. Introduction

Solid-state fluorescence has currently attracted considerable attention because of wide potentials in material science [1–3] and biology [4–6]. Recent reports highlighted the use of fluorescent nanocrystals of small organic molecules as biochips [7,8] or sensors [9–11] for applications in bioimage or biomolecules detection. Solid-state fluorescence exhibits much higher photostability than isolated dissolved molecules [12,13], and the crystal structure also favors the delocalization of the fluorescence excitation leading to unique fluorescent transmitters behavior [14]. Such properties greatly enhance the fluorescence contrast over the biological media thus lowering the thresholds of detection. However, most organic fluorophores exhibit strong fluorescence in dilute solutions but no or weak fluorescence in the solid state as a consequence of the tight molecular packing in the pure microcrystalline state or amorphous solid phase (thin film) that usually leads to significant molecular interactions and self-quenching [15,16]. Although a few of notable solid-state fluorescent families have been developed [17–21], finding a new family of solid-state fluorophores continues to be an active research area [22–26]. In this paper, we report a class of solid-state fluorophores based on dicyanoisophorone. It is found that dicyanoisophorone derivatives (Scheme 1) show moderate

fluorescence in pure state with large Stokes shifts, and with a strong push–pull chromophores dicyanoisophorone system, orange and red solid-state fluorescence are obtained.

## 2. Experimental

### 2.1. General

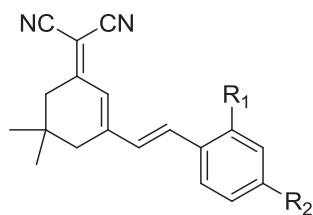
<sup>1</sup>H and <sup>13</sup>C NMR spectra are recorded at 400 and 100 MHz, respectively, with TMS as an internal reference. MS spectra are recorded with TOC-MS spectrometer, respectively. UV absorption spectra and fluorescence spectra in solution are measured with an absorption spectrophotometer (Hitachi U-3010) and a fluorescence spectrophotometer (F-2500), respectively. Fluorescence quantum yields in solid state are measured with a fluorescence spectrophotometer (Edinburgh Instruments FLS-920). All chemicals for synthesis are purchased from commercial suppliers, and solvents are purified according to standard procedures. Reaction is monitored by TLC silica gel plates (60F-254). Column chromatography is performed on silica gel (70–230 mesh).

### 2.2. Chemical

#### 2.2.1. Synthesis of 2-(3,5,5-trimethylcyclohex-2-enylidene) malononitrile

To a solution of isophorone (3.8 g, 27.6 mmol) and malononitrile (1.82 g, 27.6 mmol) in dry ethanol (150 mL) is added piperidine

\* Corresponding author. Tel.: +86 10 8254 3595; fax: +86 10 6487 9375.  
E-mail address: [yichen@mail.ipc.ac.cn](mailto:yichen@mail.ipc.ac.cn) (Y. Chen).



Scheme 1. Chemical structure of target compound.

(23 mg, 0.276 mmol). The solution is stirred at 60 °C till starting material disappeared (detected by TLC plate). After cooling to room temperature, the solution is slowly poured into water (200 mL) and the precipitated solid is filtered. Recrystallization from heptane affords a brown solid. Yield: 4.5 g (90%). M.p. 73–75 °C. <sup>1</sup>H NMR (CDCl<sub>3</sub>): δ (ppm) 6.60 (s, 1H), 2.53 (s, 2H), 2.14 (s, 2H), 2.01 (s, 3H), 1.32 (s, 6H). <sup>13</sup>C NMR (CDCl<sub>3</sub>): δ (ppm) 170.3, 161, 120.2, 113.1, 76.4, 45.6, 42.3, 32.4, 27.5, 25.1.

### 2.2.2. General synthesis of dicyanoisophorone derivatives 1–5

Under argon, 2-(3,5,5-trimethylcyclohex-2-enylidene) malononitrile (1.0 equiv.) and corresponding aromatic aldehydes (1.0 equiv.) are dissolved in dry acetonitrile (100 mL). Piperidine (0.01 equiv) is added and the solution is stirred at 40 °C till starting material disappeared (detected by TLC plate). The solution is concentrated and the product is purified by flash column chromatography (elute: petroleum ether/ethyl acetate = 10/1, v/v).

**1.** Yield: 26%. <sup>1</sup>H NMR (400 MHz, CDCl<sub>3</sub>): δ = 7.68 (d, *J* = 8.9 Hz, 2H), 7.47 (m, 2H), 7.33 (m, 1H), 7.01 (d, *J* = 16 Hz, 1H), 6.84 (d, *J* = 16 Hz, 1H), 6.73 (s, 1H), 2.56 (s, 2H), 2.44 (s, 2H), 1.20 (s, 6H). <sup>13</sup>C NMR (100 MHz, CDCl<sub>3</sub>): δ = 169.2, 153.8, 137.0, 135.6, 129.7, 129.1, 129.0, 127.5, 123.5, 113.4, 112.6, 111.6, 78.7, 43.0, 39.2, 32.0, 28.1. HRMS (EI) calcd for C<sub>19</sub>H<sub>18</sub>N<sub>2</sub> (M<sup>+</sup>): 274.1470. Found: 274.1474. Anal. Calcd for C<sub>19</sub>H<sub>18</sub>N<sub>2</sub>: C, 83.18; H, 6.61. Found: C, 83.03; H, 6.57. IR (KCl, cm<sup>-1</sup>): 2212, 1387, 1202, 1157, 962, 874.

**2.** Yield: 30%. <sup>1</sup>H NMR (400 MHz, CDCl<sub>3</sub>): δ = 7.78 (d, *J* = 8.9 Hz, 2H), 7.18 (d, *J* = 8.9 Hz, 2H), 7.04 (d, *J* = 16 Hz, 1H), 6.82 (d, *J* = 16 Hz, 1H), 6.74 (s, 1H), 3.94 (s, 3H), 2.54 (s, 2H), 2.42 (s, 2H), 1.21 (s, 6H). <sup>13</sup>C NMR (100 MHz, CDCl<sub>3</sub>): δ = 169.4, 162.5, 159.2, 155.4, 132.2, 128.8, 127.2, 122.3, 117.9, 113.9, 113.2, 105.6, 98.5, 76.9, 55.6, 55.5, 43.1, 39.2, 32, 28. HRMS (EI) calcd for C<sub>20</sub>H<sub>20</sub>N<sub>2</sub>O (M<sup>+</sup>): 304.1576. Found: 304.1571. Anal. Calcd for C<sub>20</sub>H<sub>20</sub>N<sub>2</sub>O: C, 78.92; H, 6.62.

Found: C, 80.05; H, 6.59. IR (KCl, cm<sup>-1</sup>): 2212, 1387, 1200, 1157, 954, 873.

**3.** Yield: 37%. <sup>1</sup>H NMR (400 MHz, CDCl<sub>3</sub>): δ = 7.70 (d, *J* = 9.1 Hz, 2H), 7.58 (d, *J* = 9.0 Hz, 2H), 7.05 (d, *J* = 16 Hz, 1H), 6.80 (d, *J* = 16 Hz, 1H), 6.72 (s, 1H), 2.53 (s, 2H), 2.40 (s, 2H), 1.22 (s, 6H). <sup>13</sup>C NMR (100 MHz, CDCl<sub>3</sub>): δ = 169.8, 162.9, 160.2, 157.4, 133.2, 129.8, 129.2, 122.9, 118.3, 114.4, 113.9, 110.5, 102.5, 78.6, 55.3, 43.1, 39.3, 32.1, 28.4. HRMS (EI) calcd for C<sub>19</sub>H<sub>17</sub>ClN<sub>2</sub> (M<sup>+</sup>): 308.1080. Found: 308.1085. Anal. Calcd for C<sub>19</sub>H<sub>17</sub>ClN<sub>2</sub>: C, 73.90; H, 5.55. Found: C, 74.05; H, 5.69. IR (KCl, cm<sup>-1</sup>): 2212, 1387, 1196, 1153, 960, 873.

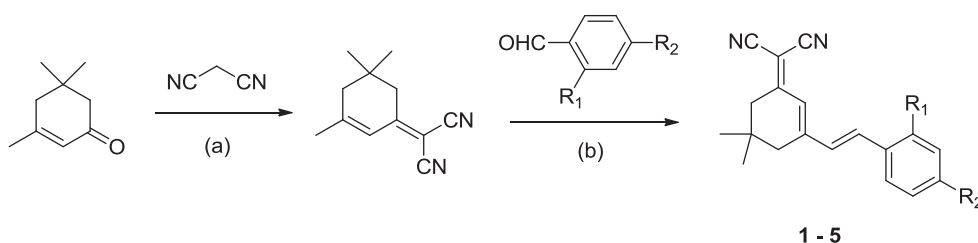
**4.** Yield: 66%. <sup>1</sup>H NMR (400 MHz, CDCl<sub>3</sub>): δ = 8.04 (d, *J* = 9.4 Hz, 1H), 7.11 (d, *J* = 7.9 Hz, 1H), 7.06 (d, *J* = 16 Hz, 1H), 6.83 (d, *J* = 16 Hz, 1H), 6.73 (s, 1H), 6.68 (s, 1H), 4.01 (s, 3H), 3.94 (s, 3H), 2.52 (s, 2H), 2.41 (s, 2H), 1.19 (s, 6H). <sup>13</sup>C NMR (100 MHz, CDCl<sub>3</sub>): δ = 169.2, 161.0, 154.3, 136.8, 129.1, 128.3, 126.8, 122.5, 114.4, 113.6, 112.9, 77.5, 55.3, 42.9, 39.1, 31.9, 27.9. HRMS (EI) calcd for C<sub>21</sub>H<sub>22</sub>N<sub>2</sub>O<sub>2</sub> (M<sup>+</sup>): 334.1681. Found: 334.1678. Anal. Calcd. For C<sub>21</sub>H<sub>22</sub>N<sub>2</sub>O<sub>2</sub>: C, 75.42; H, 6.63. Found: C, 75.55; H, 6.53. IR (KCl, cm<sup>-1</sup>): 2193, 1381, 1196, 967, 876.

**5.** Yield: 50%. <sup>1</sup>H NMR (400 MHz, CDCl<sub>3</sub>): δ = 7.38 (d, *J* = 8.9 Hz, 2H), 7.01 (d, *J* = 16 Hz, 1H), 6.76 (d, *J* = 16 Hz, 1H), 6.73 (s, 1H), 6.64 (d, *J* = 8.9 Hz, 2H), 3.12 (s, 6H), 2.74 (s, 2H), 2.65 (s, 2H), 1.06 (s, 6H). <sup>13</sup>C NMR (100 MHz, CDCl<sub>3</sub>): δ = 169.2, 155.3, 151.2, 138.3, 129.5, 129.4, 124.4, 121.4, 114.1, 113.4, 112.3, 75.7, 42.9, 40.3, 39.2, 31.8, 28.1. HRMS (EI) calcd for C<sub>21</sub>H<sub>24</sub>N<sub>3</sub> (M<sup>+</sup>+1): 318.1970. Found: 318.1889. Anal. Calcd. For C<sub>21</sub>H<sub>23</sub>N<sub>3</sub>: C, 79.46; H, 7.30. Found: C, 79.65; H, 7.18. IR (KCl, cm<sup>-1</sup>): 2196, 1389, 1205, 1163, 957, 872.

## 3. Results and discussion

### 3.1. Synthesis of dicyanoisophorone derivatives 1–5

Dicyanoisophorone derivatives are obtained starting from isophorone, malononitrile and the corresponding aromatic aldehydes by a double Knoevenagel reaction sequence [27]. Compounds 1–5 were prepared by a two-step condensation reaction [28] which illustrated in Scheme 2. Treatment isophorone with malononitrile in the catalyst of piperidine (1% mol) provided 2-(3,5,5-trimethylcyclohex-2-en-1-ylidene) malononitrile in excellent yield (90%, isolated yield), followed by the condensation with the corresponding aromatic aldehydes to give target compounds 1–5 in 33–66% isolated yield after column chromatography. The details of procedure for the preparation are described in Experimental Section.



- 1:** R<sub>1</sub> = H, R<sub>2</sub> = H  
**2:** R<sub>1</sub> = H, R<sub>2</sub> = OMe  
**3:** R<sub>1</sub> = H, R<sub>2</sub> = Cl  
**4:** R<sub>1</sub> = OMe, R<sub>2</sub> = OMe  
**5:** R<sub>1</sub> = H, R<sub>2</sub> = NMe<sub>2</sub>

Scheme 2. General synthetic route for dicyanoisophorone derivatives 1–5. Reagents and conditions: (a) piperidine cat., dry ethanol, 60 °C, 8 h, 90%; (b) piperidine cat., dry acetonitrile, 40 °C, 8 h, 33–66%.

### 3.2. Optical properties of dicyanoisophorone derivatives 1–5 in solution

The optical properties of dicyanoisophorone derivatives 1–5 are measured in CH<sub>3</sub>CN solution (20 μM) and photophysical data are reported in Table 1. Absorbance and fluorescence spectra of the representative compounds 1–5 measured at room temperature are shown in Fig. 1 and Fig. 2, respectively. Absorption data are characteristic of induced charge transfer transitions in push–pull dipolar molecules. It is found that the maximum absorption shifts from 386 nm to 492 nm when electron-donating substituents change from Cl (weak) to NMe<sub>2</sub> (strong), which is in agreement with the assumption of intramolecular charge transfer (ICT), and an ICT enhancement results in the bathochromic shift of the absorption bands.

Dicyanoisophorone derivatives 1–5 show weak fluorescence in solution. Fluorescence quantum yields ( $\phi_f$ ) are measured in CH<sub>3</sub>CN solution using rubrene ( $\phi_f = 0.27$ , in MeOH) as reference [29]. As presented in Table 1, A significant dependence of the fluorescence quantum yield with substituents is observed. It is found that the fluorescence of dicyanoisophorone derivatives is increased with increase of the power of donor, the largest fluorescence quantum yield ( $\phi_f = 0.11$ ) is obtained when substituent is *N,N*-dimethylamino donor group, which indicates that the fluorescence of dicyanoisophorone derivatives is increased with the increase of ICT in push–pull dicyanoisophorone molecules. Besides, the emission bands of 1–5 are also significant bathochromic shift with increase of ICT, the maximum emission shifts from 507 nm to 643 nm when substituent changed from Cl to NMe<sub>2</sub>.

Large Stoke's shifts are observed with dicyanoisophorone derivatives 1–5 in solution. As presented in Table 1, more than 4000 cm<sup>-1</sup> ( $\Delta\lambda \geq 119$  nm) of Stokes shift is obtained with electron-donating group (most current fluorophores only have 50–90 nm of Stoke's shift [22,30]). Such a large Stoke's shift is beneficial to such a large Stoke's shift is beneficial to application since it reduces self-absorption of fluorescent dye and prevents the decrease of fluorescence.

Both absorption and fluorescence of dicyanoisophorone derivatives 1–5 in different solvents have also been measured. As presented in Fig. 3 and Fig. 4, a positive solvatochromism of 2 is observed in different solvent. Both absorption and fluorescence occurred red-shift 20 nm and 50 nm, respectively, when the solvent is changed from cyclohexane to DMSO. Similar results were obtained when other dicyanoisophorone derivatives were measured in different solvents. The solvatochromism is characteristic of induced charge transfer transitions in push–pull dipolar molecules, which is in agreement with this attribution and in agreement with reported in this type of molecules [23].

**Table 1**  
Spectroscopic data of compounds 1–5 in CH<sub>3</sub>CN solution.<sup>a</sup>

Compds	$\lambda_{\max}$ (nm)	$\epsilon$ ( $\lambda_{\max}$ ) (l cm <sup>-1</sup> mol <sup>-1</sup> )	$\lambda_{\text{em}}$ (nm)	$\phi_f$	$\Delta\lambda$ (nm)	$\Delta\nu$ (cm <sup>-1</sup> )
1	386	26,900	505	0.01	119	6104
2	412	37,550	556	0.03	144	6286
3	386	44,650	507	0.01	121	6182
4	426	41,500	571	0.04	145	5961
5	492	21,700	643	0.11	151	4773

<sup>a</sup>  $\lambda_{\text{abs}}$ : maximum absorption wavelength,  $\lambda_{\text{em}}$ : maximum emission wavelength at ambient temperature,  $\epsilon$ : molar absorption coefficients at maximum absorption wavelength,  $\Delta\lambda$ : Stoke's shift calculated by ( $\Delta\lambda = \lambda_{\text{em}} - \lambda_{\text{abs}}$  nm),  $\Delta\nu$ : Stoke's shift calculated by [ $\Delta\nu = (1/\lambda_{\text{max}} - 1/\lambda_{\text{em}}) \times 10^7$  cm<sup>-1</sup>],  $\phi_f$ : fluorescence quantum yield using rubrene ( $\phi_f = 0.27$ , in MeOH) as reference.

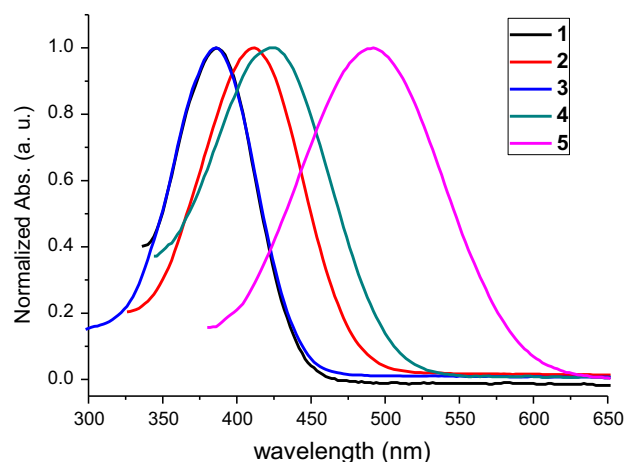


**Fig. 1.** The absorption of 1–5 in CH<sub>3</sub>CN solution.

### 3.3. Fluorescence of dicyanoisophorone derivatives 1–5 in pure microcrystalline state

Both absorption and fluorescence of dicyanoisophorone derivatives 1–5 in pure solid state are measured. Relevant photophysical data are summarized in Table 2 and normalized fluorescence spectra of dicyanoisophorone derivatives 1–5 is shown in Fig. 5. It is found that the maximum absorption shifted from 418 nm to 528 nm when substituent changed from Cl group to NMe<sub>2</sub> group in a push–pull dicyanoisophorone structure, which is in agreement with the result in solution. Solid-state fluorescence of dicyanoisophorone derivatives 1–5 have showed that all compounds exhibited fluorescence emission in pure solid state. The quantum yields of derivatives 1–5 in solid state are measured by an integrating sphere and the largest quantum yield of  $\phi = 0.15$  are obtained (Table 2). As compared to solution, the fluorescence of dicyanoisophorone derivatives 1–4 in solid state is stronger than that in solution but 5 (whose fluorescence is small as compared to in the solution). An enhancement of fluorescence of derivatives 1–4 in solid state probably resulted from the aggregation-induced emission or the aggregation-induced emission enhancement due to the effects of intramolecular planarization or restricted intramolecular vibrational and rotational motions in the solid state or of specific aggregation or certainly a combination of all those effects [31,32].

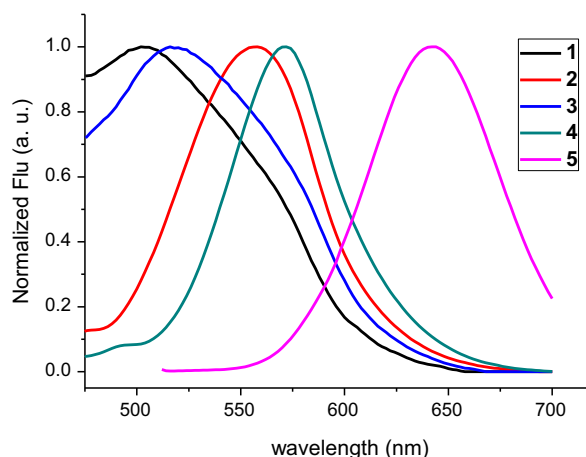


**Fig. 2.** The fluorescence of 1–5 in CH<sub>3</sub>CN solution.

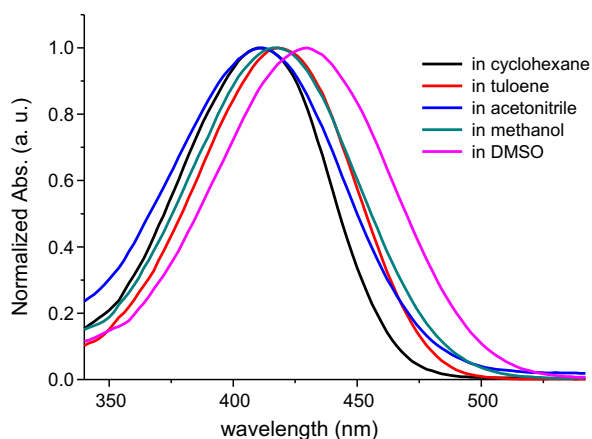


Fig. 3. The absorption of **2** in different solution.

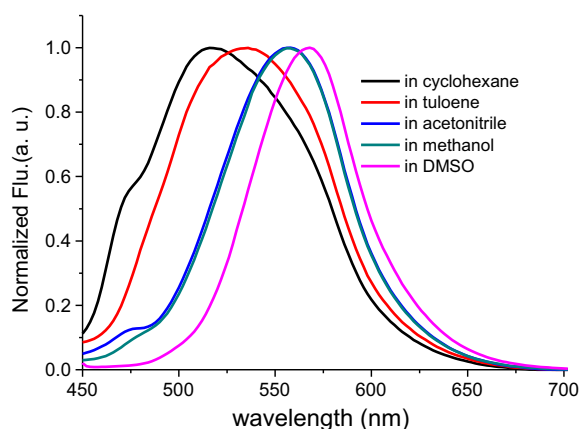


Fig. 4. The fluorescence of **2** in different solution.

To insight into a possible mechanism for the enhancement of fluorescence of dicyanoisophorone derivatives in solid state, aggregation behaviors of derivatives **1–5** in tetrahydrofuran (THF) and water (H<sub>2</sub>O) mixed solvent are investigated. As presented in Fig. 6, the fluorescence intensity of **2** was enhanced continually with a red-shift from 549 nm to 571 nm until the water was added up to 80% (volume ratio). The observed continuous emission enhancement and red-shift might arise from the concerted effect of an increase in the polarity of water and the resultant self-assembled agglomerates, which is similar with a polymer character [33,34]. Similar results were obtained when other derivatives **1, 3** and **4** were measured in mixed solvent. It is worth noting that, a opposite result was obtained when **5** was investigated in mixed

**Table 2**  
Spectroscopic data of compounds **1–5** in pure microcrystalline state.<sup>a</sup>

Compds	$\lambda_{\text{abs}}$ (nm)	$\lambda_{\text{em}}$ (nm)	$\phi_f$	$\Delta\lambda$ (nm)	$\Delta\nu$ (cm <sup>-1</sup> )
<b>1</b>	435	558	0.01	123	5067
<b>2</b>	446	576	0.13	130	5060
<b>3</b>	418	541	0.07	123	5439
<b>4</b>	459	592	0.15	133	4894
<b>5</b>	528	670	0.003	142	4014

<sup>a</sup>  $\lambda_{\text{abs}}$ : maximum absorption wavelength,  $\lambda_{\text{em}}$ : maximum emission wavelength at ambient temperature,  $\phi_f$ : measured by an integrating sphere at ambient temperature,  $\Delta\lambda$ : Stoke's shift calculated by ( $\Delta\lambda = \lambda_{\text{em}} - \lambda_{\text{abs}}$  nm),  $\Delta\nu$ : Stoke's shift calculated by [ $\Delta\nu = (1/\lambda_{\text{max}} - 1/\lambda_{\text{em}}) \times 10^7$  cm<sup>-1</sup>].

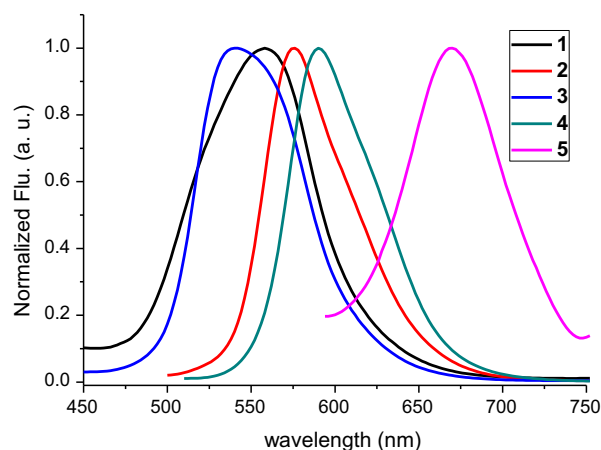


Fig. 5. Fluorescence spectral of **1–5** in pure solid state.

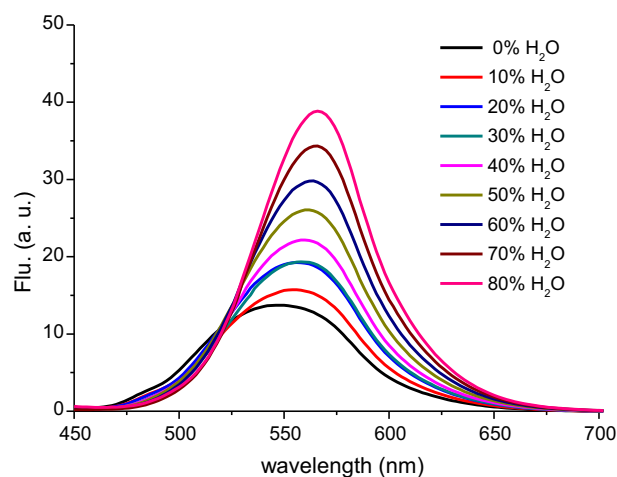


Fig. 6. Fluorescence spectral of **2** in mixed solvent (THF–water).

solvent, as shown in Fig. 7, the fluorescence intensity was decreased continually with increase of water, which indicated that the aggregation of **5** caused its fluorescence quenching (the result is agreement with the fluorescence quantum yield of **5** in solid state). The different results suggested that the controlled crystalline

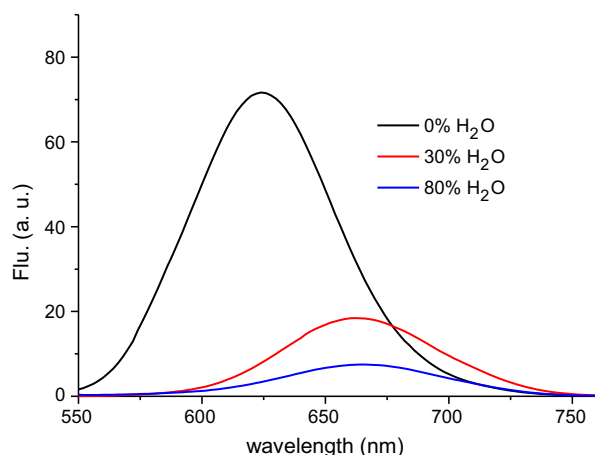


Fig. 7. Fluorescence spectral of **5** in mixed solvent (THF–water).

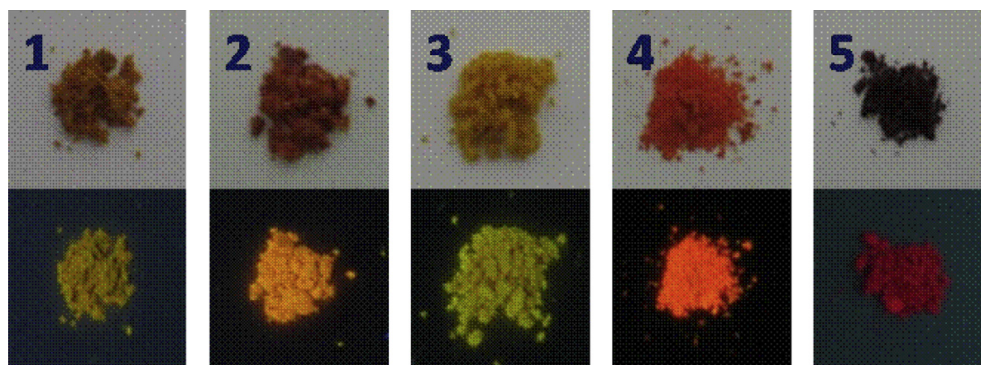


Fig. 8. Photograph of 1–5 in pure solid state (top) and their solid-state under illumination of handled UV lamp at 365 nm (bottom).

engineering through different molecular stacking might play a great role in the different macroscopic solid state emission behaviors [20].

Similar to solution, a large red-shift of emission is observed when substituents changed from Cl group to  $\text{NMe}_2$  group and large Stoke's shift are obtained with dicyanoisophorone derivatives 1–5 in pure solid state, which suggests that ICT also took place in dicyanoisophorone molecules in pure solid state. With a strong electron-donating group, both red and orange solid-state fluorescence of dicyanoisophorone derivatives are obtained (Fig. 8).

#### 4. Conclusions

In summary, a class of fluorophores based on dicyanoisophorone derivatives has been developed. It has demonstrated that dicyanoisophorone derivatives exhibit fluorescence in both solution and pure solid state with large Stokes shifts. It has also demonstrated that electronic property of substituents has greatly effected on the optical properties of dicyanoisophorone derivatives, with a strong push–pull chromophores dicyanoisophorone system, a red or orange solid-state fluorescence is obtained.

#### Acknowledgments

This work was supported by the National Natural Science Foundation of China (No 91123032) and National Basic Research Program of China (2010CB934103).

#### References

- [1] Dong YQ, Lam JWY, Qin AJ, Liu JZ, Li Z, Tang BZ. Excimer laser annealing of silicon nanowires. *Appl Phys Lett* 2007;91:11111–3.
- [2] Wang M, Zhang G, Zhang D, Zhu D, Tang BZ. Fluorescent bio/chemosensors based on silole and tetraphenylethene luminogens with aggregation-induced emission feature. *J Mater Chem* 2010;20:1858–67.
- [3] Lu H, Xu B, Dong Y, Chen F, Li Y, Li Z, et al. Novel fluorescent pH sensors and a biological probe based on anthracene derivatives with aggregation-induced emission characteristics. *Langmuir* 2010;26:6838–44.
- [4] Huang J, Wang M, Zhuo Y, Weng X, Shuai L, Zhuo X, et al. Visual observation of G-quadruplex DNA with the label-free fluorescent probe silole with aggregation-induced emission. *Bioorg Med Chem* 2009;17:7743–8.
- [5] Liu Y, Deng CM, Tang L, Qin AJ, Hu RR, Sun JZ, et al. Specific detection of d-glucose by a tetraphenylethene-based fluorescent sensor. *J Am Chem Soc* 2011;133:660–3.
- [6] Shiraishi K, Sanji T, Tanaka M. A new fluorescent sensor for the detection of pyrophosphate based on a tetraphenylethylene moiety. *Tetrahedron Lett* 2010;51:1960–2.
- [7] Zhao X, Tapeç-Dytioco R, Tan W. Ultrasensitive DNA detection using highly fluorescent bioconjugated nanoparticles. *J Am Chem Soc* 2003;125:11474–5.
- [8] Dubuisson E, Monnier V, Sanz-Menez N, Boury B, Usson Y, Pansu RB, et al. Brilliant molecular nanocrystals emerging from sol–gel thin films: towards a new generation of fluorescent biochips. *Nanotechnology* 2009;20:315301–7.
- [9] Wang L, Wang L, Dong L, Bian G, Xia T, Chen H. Direct fluorimetric determination of  $\gamma$ -globulin in human serum with organic nanoparticle biosensor. *Spectrochim Acta A Mol Biomol Spectrosc* 2005;61:129–33.
- [10] Chan CPY, Tzang LCH, Sin KK, Ji SI, Cheung KY, Tam TK, et al. Biofunctional organic nanocrystals for quantitative detection of pathogen deoxyribonucleic acid. *Anal Chim Acta* 2007;584:7–11.
- [11] Sabella S, Brunetti V, Vecchio G, Della Torre A, Rinaldi R, Cingolani R, et al. Micro/nanoscale parallel patterning of functional biomolecules, organic fluorophores and colloidal nanocrystals. *Nanoscale Res Lett* 2009;4:1222–9.
- [12] Kim HY, Bjirkklund TG, Lim SH, Bardeen CJ. Spectroscopic and photocatalytic properties of organic tetracene nanoparticles in aqueous solution. *Langmuir* 2003;19:3941–6.
- [13] Sanz N, Ibanez A, Morel Y, Baldeck PL. Organic nanocrystals grown in gel glasses for optical-power-limiting applications. *Appl Phys Lett* 2001;78:2569–71.
- [14] Botzung-Appert E, Monnier V, Duong TH, Pansu R, Ibanez A. Polyaromatic luminescent nanocrystals for chemical and biological sensors. *Chem Mater* 2009;21:1609–11.
- [15] An BK, Kwon SK, Jung SD, Park SY. Enhanced emission and its switching in fluorescence organic nanoparticles. *J Am Chem Soc* 2002;124:14410–5.
- [16] Tracy HJ, Mullin JL, Klooster WT, Martin JA, Haug J, Wallace S, et al. Enhanced photoluminescence from group 14 metalloids in aggregated and solid solutions. *Inorg Chem* 2005;44:2003–11.
- [17] Luo JD, Xie ZL, Lam JWY, Cheng L, Chen HY, Qiu CF, et al. Aggregation-induced emission of 1-methyl-1,2,3,4,5-pentaphenylsilole. *Chem Commun* 2001;18:1740–1.
- [18] Wu CC, Lin YT, Wong KT, Chen YY. Efficient organic blue-light-emitting devices with double confinement on terfluorenes with ambipolar carrier transport properties. *Adv Mater* 2004;16:61–5.
- [19] Sartin MM, Boydston AJ, Pagenkopf BL, Bard AJ. Electrochemistry, spectroscopy, and electrogenerated chemiluminescence of silole-based chromophores. *J Am Chem Soc* 2006;128:10163–70.
- [20] Shi C, Guo Z, Yan Y, Zhu S, Xie Y, Zhao YS, et al. Self-assembly solid-state enhanced red emission of quinolinemalononitrile: optical waveguides and stimuli response. *ACS Appl Mater Interfaces* 2013;5:192–8.
- [21] Guo Z, Zhu W, Tian H. Dicyanomethylene-4H-pyran chromophores for OLED emitters logic gates and optical chemosensors. *Chem Commun* 2012;48:6073–84.
- [22] Ozdemir T, Atilgan S, Kutuk I, Serdar Yildirim S, Tulek A, Bayindir M, et al. Solid-state emissive BODIPY dyes with bulky substituents as spacers. *Org Lett* 2009;11:2105–7.
- [23] Massin J, Dayoub W, Mulatier JC, Aronica C, Bretonniere Y, Andraud C. Near-infrared solid-state emitters based on isophorone: synthesis, crystal structure and spectroscopic properties. *Chem Mater* 2011;23:862–73.
- [24] Wang J, Mei J, Yuan WZ, Lu P, Qin AJ, Sun JZ, et al. Hyperbranched polytriazoles with high molecular compressibility: aggregation-induced emission and superamplified explosive detection. *J Mater Chem* 2011;21:4056–9.
- [25] Hu XM, Chen Q, Zhou D, Cao J, He YJ, Han BH. One-step preparation of fluorescent inorganic–organic hybrid material used for explosive sensing. *Polym Chem* 2011;2:1124–8.
- [26] Liu Y, Yu Y, Lam JWY, Hong Y, Faisal M, Yuan WZ, et al. Simple biosensor with high selectivity and sensitivity: thiol-specific biomolecular probing and intracellular imaging by AIE fluorogen on a TLC plate through a thiol–ene click mechanism. *Chem Eur J* 2010;16:8433–8.
- [27] Lemke R. Knoevenagel-Kondensationen in Dimethylformamid. *Synthesis* 1974;5:359–61.

- [28] Kleinpeter E, Koch A, Mikhova B, Stamboliyska BA, Kolev T. Quantification of the push–pull character of the isophorone chromophore as a measure of molecular hyperpolarizability for NLO applications. *Tetrahedron Lett* 2008;49:1323–7.
- [29] Boens N, Qin W, Basari N, Hofkens J, Ameloot M, Pouget J, et al. Fluorescence lifetime standards for time and frequency domain fluorescence spectroscopy. *Anal Chem* 2007;79:2137–49.
- [30] Langhals H, Krotz O, Polborn K, Mayer P. A novel fluorescent dye with strong anisotropic solid-state fluorescence, small Stokes shift, and high photostability. *Angew Chem Int Ed Engl* 2005;44:2427–8.
- [31] Tang BZ, Zhan XW, Yu G, Lee PPS, Liu YQ, Zhu DB. Efficient blue emission from siloles. *J Mater Chem* 2001;11:2974–8.
- [32] Hong YN, Lam JWY, Tang BZ. Aggregation-induced emission: phenomenon, mechanism and applications. *Chem Commun* 2009:4332–5.
- [33] Yuan WZ, Yu Z, Lu P, Deng C, Lam JWY, Wang Z, et al. High efficiency luminescent liquid crystal: aggregation-induced emission strategy and biaxially oriented mesomorphic structure. *J Mater Chem* 2012;22:3323–6.
- [34] Tong H, Hong Y, Dong Y, Ren Y, Haussler M, Lam JWY, et al. Color-tunable, aggregation-induced emission of a butterfly-shaped molecule comprising a pyran skeleton and two cholesteryl wings. *J Phys Chem B* 2007;111:2000–7.